Rapid Assessment of Cardiac Function Using 2D CINE SSFP in Conjunction with k-t BLAST and k-t SENSE

T. Niendorf[1], M. Katoh[1], H. P. Kuehl[2], H. Grawe[2], J. Bunke[3], M. Kouwenhoven[3], R. W. Guenther[1]

[1]Department of Diagnostic Radiology, University of Aachen, University Hospital, Aachen, Germany, [2]Department of Cardiology, University of Aachen, University Hospital, Aachen, Germany, [3]Clinical Science, Philips Medical Systems, Best, Netherlands

Purpose

In current clinical practice CINE imaging for the assessment of left ventricular (LV) function is generally confined to 1 slice per breath-hold due to the competing constraints of acquisition time, spatial and temporal resolution and signal-to-noise ratio (SNR). With 8 to 10 short axis slices required to cover the heart the conventional approach results in prolonged examination times of app. 10 minutes, with corresponding patient discomfort. Parallel imaging can overcome these difficulties by allowing 3D acquisitions at the expense of temporal and spatial resolution (1). For this reason, a strategy employing accelerated 2D CINE techniques encompassing 3-4 slices per breath-hold (BH) is conceptually appealing for the pursuit of comprehensive heart coverage in clinically acceptable examination times. To approach this goal, this study examines the applicability of accelerated 2D CINE SSFP imaging for global LV function assessment. To achieve high accelerations supporting the extended slice coverage without prohibitive noise amplification associated with coil sensitivity encoding (SENSE), spatio-temporal correlations in dynamic CINE imaging are exploited using *k-t* BLAST and *k-t* SENSE (2).

Methods

2D CINE imaging was conducted in 12 healthy adult volunteers (mean=35 ± 5 years) using a 1.5 Tesla MR system (Philips, Best, Netherlands) together with a 5-element cardiac phased array coil. An ECG-gated 2D SSFP pulse sequence (TE=1.85 ms, TR=3.7 ms, α=60°, FOV = (35x35) cm^2, slice thickness=8 mm, matrix =192×192 (reconstructed 384x384), cardiac phases=25) was customized to support parallel imaging using SENSE (3), *k-t* BLAST and *k-t* SENSE (2). Aliasing in the undersampled *k-t* data was resolved using signal correlations obtained from integrated low resolution training data (4). Coil sensitivity calibration was accomplished using an extra reference scan. Accelerated breath-held (end-expiration) CINE imaging was conducted using three different strategies: (i) SENSE imaging (R=2.5, 3 slices/BH), (ii) *k-t* BLAST/*k-t* SENSE (R=5, 3 slices/BH) and (iii) *k-t* BLAST/k-t SENSE (R=8, 4 slices/BH). For comparison conventional 2D CINE SSFP imaging (single slice/BH) was carried out. For quantification end-diastolic and end-systolic volume (EDV, ESV), stroke volume (SV), ejection fraction (EF), and the left ventricular mass (LVM) were determined. M-mode like 1D projections through the short axis views (dotted lines in Fig. 1) were generated using IDL (RSI, Bolder, Co, USA). Myocardial border edge detection was performed using Derich edge detection filter (5). Myocardial border sharpness (aMBS) was defined as the average edge value along the calculated myocardial border.

Results

Short axis views demonstrate the quality of the unfolded images as well as the level of contrast achieved with conventional and accelerated 2D CINE SSFP (Fig. 1, top). The total examination time was 173±15 s for the SENSE approach (R=2.5), 178±15 s for the 5-fold and 160±15 s for the 8- fold accelerated *k-t* approach. The conventional approach revealed a total examination time of app. 9 min. The LV function parameter obtained from the SENSE acquisitions (R=2.5) were in agreement with those derived from the conventional approach (Tab. 1). The *k-t* approach yielded LV parameter which were statistically different from those obtained for the conventional approach with the exception of left ventricular mass (Tab.1). However, the difference between the conventional and 5-fold accelerated *k-t* approach was considered to be clinically irrelevant. Use of (i) SENSE (R=2.5) and (ii) 5-fold accelerated *k-t* techniques did allow sufficiently high effective temporal resolution to achieve very well delineated myocardial borders as shown in Fig. 1b-d. The myocardial borders sharpness was found to be diminished for the 8-fold accelerated *k-t* approach (Fig. 1e,f). This resulted in an apparent increase in the myocardial wall thickness which was pronounced at systole.

		conv.	SENSE (R=2.5)	*k-t* BLAST (R=5)	*k-t* SENSE (R=5)	*k-t* BLAST (R=8)	*k-t* SENSE (R=8)
EDV	mean	158±14	155±13	153±13	146±11	150±11	145±11
(ml)	p		0,31	0,001	<0,001	0,002	<0,001
ESV	mean	62±6	61±5	64±5	64±6	67±5	67±5
(ml)	p		0,48	0,242	0,103	0,002	0,005
SV	mean	95±11	94±10	88±10	82±8	82±9	77±9
(ml/hb)	p		0,74	0,003	<0,001	<0,001	<0,001
EF	mean	60±4	60±3	56±3	56±3	54±3	53±3
(%)	p		0,72	0,028	0,001	<0,001	<0,001
LVM	mean	100±11	99±11	100±11	94±9	100±12	95±10
(g)	p		0,96	0,79	0,011	0,68	0,33
aMBS	mean	0.39	0.27	0.29	0.26±	0.21	0.21

Tab 1: Physiological parameter (EDV, ESV, SV, EF, LVM) and averaged myocardial border sharpness (a,MBS, large values correspond to better delineation) derived from the left and right border of the septum.

References:
(1) Rettmann, D.W. et al., ISMRM, 541 (2004), (2) Tsao, J. et al., Magn. Reson. Med. 50, 1031 (2003), (3) Prüssmann K. et al., Magn. Reson. Med. 42, 952 (1999), (4) Kozerke, S. et al., ISMRM, 1564 (2003), (5) Deriche R. eta al., IEEE Trans PAMI, 12, 78 (1990)

Conclusions

The feasibility of robust accelerated 2D CINE SSFP imaging using spatio-temporal correlations in the dynamic data has been demonstrated and the imaging speed advantage over the conventional approach has been shown. The accelerated 2D imaging paradigm presented here promises to extend the capabilities of breath-hold CINE imaging from a single slice to multiple slices per breath-hold. Despite the clear imaging speed and SNR advantage of the *k-t* approach, myocardial border sharpness remains a challenge. Limitations in the effective temporal resolution dictate that a fairly rapid degeneration of myocardial border sharpness at accelerations larger than R=8 may be inevitable.

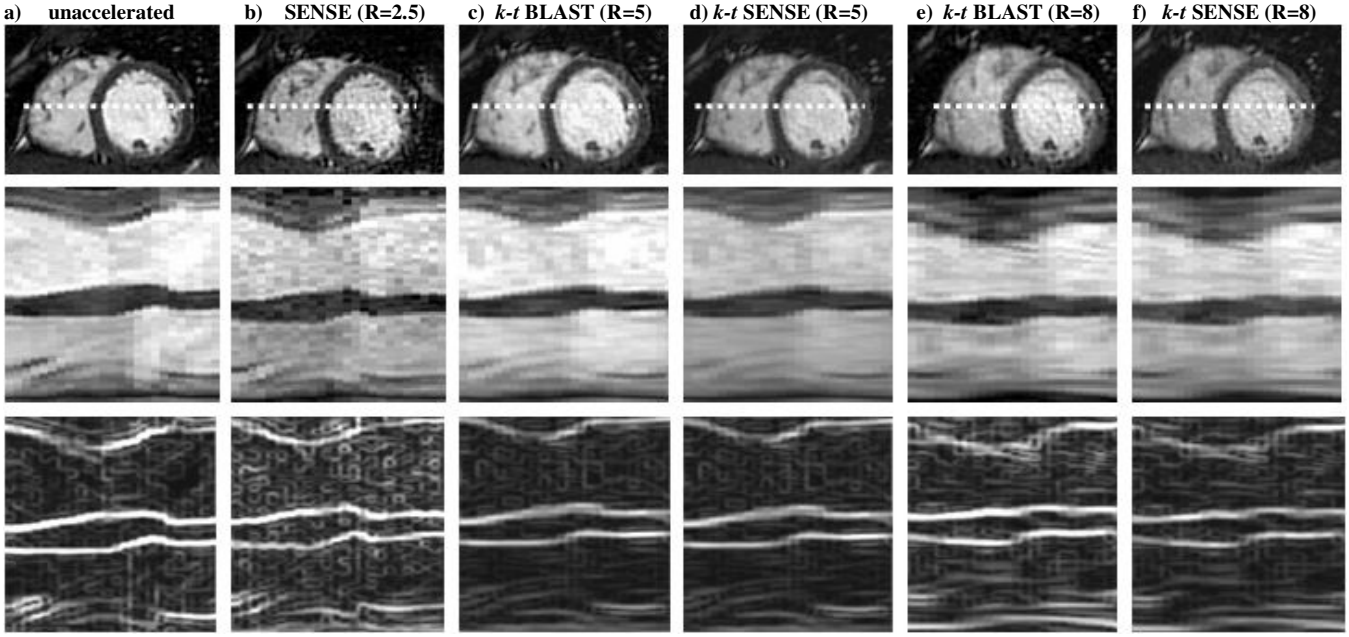

Fig. 1: Short axis views (**top**), 1D projections along dotted lines through the short axis views covering the entire R-R interval **(middle)** and images obtained from the edge detection algorithm **(bottom)**.